



# Manganite-based three level memristive devices with self-healing capability



W. Román Acevedo<sup>a,b</sup>, D. Rubi<sup>a,b,c,\*</sup>, J. Lecourt<sup>d</sup>, U. Lüders<sup>d</sup>, F. Gomez-Marlasca<sup>a</sup>, P. Granell<sup>e</sup>, F. Golmar<sup>b,c,e</sup>, P. Levy<sup>a,b</sup>

<sup>a</sup> Gerencia de Investigación y Aplicaciones, CNEA, Av. Gral Paz 1499 (1650), San Martín, Buenos Aires, Argentina

<sup>b</sup> Consejo Nacional de Investigaciones Científicas y Técnicas (CONICET), Argentina

<sup>c</sup> Escuela de Ciencia y Tecnología, UNSAM, Campus Miguelete (1650), San Martín, Buenos Aires, Argentina

<sup>d</sup> CRISMAT, CNRS UMR 6508, ENSICAEN, 6 Boulevard Maréchal Juin, 14050 Caen Cedex 4, France

<sup>e</sup> INTI – CMNB, Av. Gral Paz 5445 (B1650KNA), San Martín, Buenos Aires, Argentina

## ARTICLE INFO

### Article history:

Received 14 March 2016

Received in revised form 12 June 2016

Accepted 16 June 2016

Available online 21 June 2016

Communicated by L. Ghivelder

### Keywords:

RRAM devices

Resistive switching

Manganites

## ABSTRACT

We report on non-volatile memory devices based on multifunctional manganites. The electric field induced resistive switching of Ti/La<sub>1/3</sub>Ca<sub>2/3</sub>MnO<sub>3</sub>/n-Si devices is explored using different measurement protocols. We show that using current as the electrical stimulus (instead of standard voltage-controlled protocols) improves the electrical performance of our devices and unveils an intermediate resistance state. We observe three discrete resistance levels (low, intermediate and high), which can be set either by the application of current–voltage ramps or by means of single pulses. These states exhibit retention and endurance capabilities exceeding 10<sup>4</sup> s and 70 cycles, respectively. We rationalize our experimental observations by proposing a mixed scenario where a metallic filament and a SiO<sub>x</sub> layer coexist, accounting for the observed resistive switching. Overall electrode area dependence and temperature dependent resistance measurements support our scenario. After device failure takes place, the system can be turned functional again by heating up to low temperature (120 °C), a feature that could be exploited for the design of memristive devices with self-healing functionality. These results give insight into the existence of multiple resistive switching mechanisms in manganite-based memristive systems and provide strategies for controlling them.

© 2016 Elsevier B.V. All rights reserved.

## 1. Introduction

The resistive switching (RS) mechanism displayed by certain metal–insulator–metal structures supports a new non-volatile memory technology coined as ReRAM [1–4]. For niche applications, ReRAM is a rival of other emerging replacement technologies of presently prevailing FLASH based RAM memory devices. Strong efforts have been made to fabricate structures that could exhibit RS. Typically, a metal–insulator–metal capacitor-like structure is assessed. Although many systems and materials were tested, the description of a unified physical mechanism is still a matter of debate [1–4]. Electric field induced filament formation and oxygen vacancy drift are key ingredients in most descriptions involving transition metal oxides as the insulating layer [3]. Here we focus

on a manganese oxide multifunctional compound, La<sub>1/3</sub>Ca<sub>2/3</sub>MnO<sub>3</sub> (LCMO), a unique manganite well known for its colossal magnetoresistance and intrinsic phase separation effects [5]. Manganite based RS non-volatile memory devices were shown to exhibit unique properties, either in polycrystalline [6] or thin film [7,8] format. Electronic transport in manganites is described by electron hopping between neighbor Mn sites. As this hopping is mediated by oxygen ions existing between Mn atoms, the mechanism is known as “double exchange”. Oxygen vacancies (OV<sup>+</sup>) disrupt this hopping process, and thus increase the manganite electric resistance. On the other hand, the electrode material plays a key role, determining overall resistance levels by the introduction of a naturally formed oxide layer [9] or through the migration of metallic ions (i.e. metallic filament formation) [8,10]. Besides, manganite based non-volatile memory devices exhibit multilevel capability [11] sustained on the controlled electric field drift of vacancies [12], with the ability to tune (almost) continuously the actual resistance level. Here we perform current-controlled experiments that show that Ti/LCMO/n-Si devices exhibit, in addition to these multilevel (analogic) levels, three robust non-volatile (discrete)

\* Corresponding author at: Gerencia de Investigación y Aplicaciones, CNEA, Av. Gral Paz 1499 (1650), San Martín, Buenos Aires, Argentina. Tel.: +54 11 67727059; fax: +54 11 67727121.

E-mail address: rubi@tandar.cnea.gov.ar (D. Rubi).

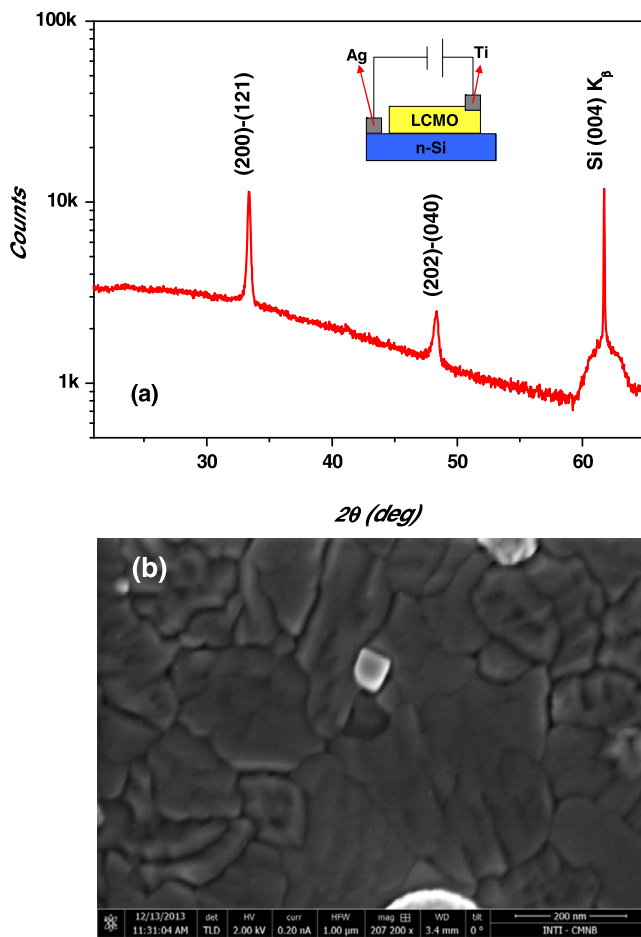


**Fig. 1.** (a) X-ray diffraction pattern corresponding to one of our LCMO thin films. The inset shows a sketch of the device electrical connection; (b) Scanning electron micrograph corresponding to the same film.

memory levels. In addition to the usual high and low resistance states, an intermediate resistance state can be stabilized. Unveiling of this three level memory device is attained through careful control of the dissipated electrical power. We elaborate on the nature of the observed RS mechanism, and propose a scenario where the experimental behavior is consistent with the existence of a Ti filament plus the oxidation/reduction of the ultrathin native  $\text{SiO}_x$  layer present at the Si-manganite interface. Finally, we show that, after device failure takes place, our devices can be turned functional again by heating them at low temperatures. The possibility of taking advantage of this fact for the design of self-healing memristive devices is discussed.

## 2. Materials and methods

LCMO manganite memory devices were grown on top of n-type silicon by pulsed laser deposition. No chemical removal of the native  $\text{SiO}_x$  layer was performed. A 266 nm Nd:YAG solid state laser, operating at a repetition frequency of 10 Hz, was used. The deposition temperature and oxygen pressure were 850 °C and 0.13 mbar, respectively. X-ray diffraction was performed by means of an Empyrean (Panalytical) diffractometer. Samples were single phase and polycrystalline, as shown in the X-ray diffraction pattern of Fig. 1(a). The manganite peaks were indexed assuming a *Pnma* orthorhombic bulk-like structure. The film thickness was estimated by focused ion beam cross-sectioning and scanning electron microscopy imaging in 100 nm. The scanning electron microscopy plane view displayed in Fig. 1(b) shows a dense microstructure

along with the presence of a small amount of particulate on the surface, which is common in pulsed laser deposited films [13]. 100 nm Ti top electrodes were deposited by sputtering and shaped by means of optical lithography. Top electrode areas ranged between  $32 \times 10^3 \mu\text{m}^2$  and  $196 \times 10^3 \mu\text{m}^2$ . Electrical characterization was performed at room temperature with a Keithley 2612 source-meter hooked to a home-made probe station. The n-type silicon substrate was grounded and used as bottom electrode. The electrical stimulus was applied to the top electrode.

## 3. Results and discussion

Electroforming polarity and strength determines most of the subsequent electrical behavior of a metal–insulator–metal structure. In a previous work on similar Ti–LCMO–nSi structures, we reported that different transport mechanisms are triggered by either positive ( $\text{F}^+$ ) or negative ( $\text{F}^-$ ) electroforming [14]. In brief,  $\text{F}^-$  determines the ulterior oxidation/reduction of the  $\text{SiO}_x$  layer at the manganite–Si interface, while  $\text{F}^+$  can be ascribed to either oxygen vacancies drift or to a metallic filament formation. Changes in the *I*–*V* curve circulation (clockwise vs. anticlockwise) with the electroforming polarity were also reported in  $\text{SrTiO}_3$  and  $\text{Ga}_2\text{O}_3$ -based systems [15,16]; however, the physical mechanisms in these cases (related to the formation of oxygen vacancies paths, which locally lower the resistance of the oxide), are substantially different from our case. Results to be discussed below were obtained applying a positive stimulus to pristine devices, namely the  $\text{F}^+$  procedure, though using the less common approach of current injection.

We started the electric testing protocol by recording pulsed voltage–current curves. Current pulses with different amplitudes ( $0 \rightarrow I_{\text{MAX}} \rightarrow -I_{\text{MIN}} \rightarrow 0$ ) and 1 ms time-width were applied. Consecutive pulses were separated by  $\sim 1$  s in order to allow the heat produced at the electrode to drain. We recall that we used the applied current as the stimulus, and voltage as the dependent variable. The rationale behind is the control of the local power release during the expected abrupt transition from the initial high resistance (HR) state to the low resistance (LR) one, the SET operation. When using the “voltage control mode” dissipated power release obeys  $P_v = V^2/R$ . While driving the device in “voltage control mode” current flow is usually limited by the apparatus internal current compliance [17,18], as a way to avoid sample damage due to the power overshoot occurring during the sudden decrease of *R* (i.e. the desired RS effect obtained through a SET operation). However, the ever limited time response of standard equipment can not avoid an unwanted overshoot. Strategies using an external device for preventing this damage include the use of a biased transistor [19] or a simple resistance [20] in series with the memory cell. An alternative strategy is the use of the “current control mode” [21], in SET operations. Thus, during a sudden decrease of *R*, the dissipated power is self-limited as power release is governed by  $P_I = I^2R$ .

Initially, all tested devices received *positive* electrical stimulus. We will focus now on the behavior of a device with area  $\sim 45 \times 10^3 \mu\text{m}^2$ . The positive electroforming process determines a sudden decrease of the resistance from the virgin ( $R_V \sim 2 \times 10^6 \Omega$ ) to the HR resistance state value ( $R_H \sim 80 \times 10^3 \Omega$ ). Next, *V*–*I* curves were performed. Upon applying a positive stimulus, the HR resistance state ( $R \sim 80 \times 10^3 \Omega$ ) can be explored for  $I < 2 \times 10^{-3}$  A. A sharp HR to LR (SET) transition occurs for  $I \sim +2 \times 10^{-3}$  A, as depicted in Fig. 2(a). When negative stimulus is explored, a transition from LR to HR (RESET) is observed to occur around  $-10 \times 10^{-3}$  A, reaching the original HR state. By cycling the stimulus between  $+17 \times 10^{-3}$  A and  $-17 \times 10^{-3}$  A, the SET–RESET operation can be repeated several times. Both HR and LR states are stable for at least  $10^4$  s (i.e. negligible decay is observed when tested using a low non-disturbing stimulus). The

Download English Version:

<https://daneshyari.com/en/article/1858882>

Download Persian Version:

<https://daneshyari.com/article/1858882>

[Daneshyari.com](https://daneshyari.com)